Vol 13 No 12, December 2004
1009-1963/2004/13(12)/2162-07

Chinese Physics

© 2004 Chin. Phys. Soc.
and IOP Publishing Ltd

Comparative study of spectroscopic properties of Er^{3+}/Yb^{3+}-codoped tellurite glass and fibres under 980nm excitation*

Dai Shi-Xun(戴世勋)†, Zhang Jun-Jie(张军杰), Li Shun-Guang(李顺光),
Xu Shi-Qing(徐时清), Wang Guo-Nian(汪国年),
Yang Jian-Hu(杨建虎), and Hu Li-Li(胡丽丽)

Shanghai Institute of Optics and Fine Mechanics, Chinese Academy of Sciences, Shanghai 201800, *China*

(Received 15 December 2003; revised manuscript received 9 June 2004)

A tellurite fibre of TeO_2–ZnO–La_2O_3–Li_2O glass codoped with 20000 ppm ytterbium and 5000 ppm erbium was fabricated by the suction casting and rod-in-tube technologies. The absorption spectrum of Er^{3+}/Yb^{3+} -codoped bulk glass has been measured. From the Judd–Ofelt intensity parameters, the spontaneous emission probability and radiative lifetime τ_{rad} of Er^{3+}:$^4I_{13/2} \rightarrow {}^4I_{15/2}$ transition for the bulk glass have been calculated. The emission fluorescence spectra and lifetimes around 1.5μm, and subsequent upconversion fluorescence in the range of 500–700nm were measured in fibres and compared with those in bulk glass. The changes in amplified spontaneous emission with fibre length and pumping power was also measured. It was found that the emission spectrum from erbium in fibres is almost twice as broad as the corresponding spectrum in bulk glass when pumped at 980nm.

Keywords: tellurite glass, fibre, erbium doping, spectroscopy, Judd–Ofelt theory
PACC: 7855, 4255R, 7840, 4280S, 3350D

1. Introduction

Recently, there has been a great interest in Er^{3+} doped tellurite glasses which can be used for 1.5μm active optical devices such as fibre-optical amplifier[1–4] and planer waveguide.[5,6] Erbium-doped tellurite fibres offer broad amplification bandwidth and high radiative transition efficiency.[1–4] They are now promising candidates for use in fabricating novel optical amplifiers as a means of extending the transmission bandwidth of optical fibres beyond the range available from conventional Er^{3+}-doped silica fibre, such as erbium-doped tellurite fibre amplifier (EDTFA) for the C-band and L-band.[1–4,7] 980nm laser diode (LD) was often used as the pumping source to realize 1.5μm amplification with broadband gain, high power output and good noise figure instead of 1480nm pumping.[8] In order to improve the pumping efficiency of 980nm LD, Yb^{3+} was used mostly as a sensitizer since it exhibits an intense broad absorption cross section between 850nm and 1080nm, while Er^{3+} has weak absorption in this band range.[9]

On the other hand, erbium-doped fibres (EDF) have recently been the focus of intensive research in amplified spontaneous emission (ASE) sources as well as optical amplifiers.[10–13] In general, an incoherent broadband optical source with low spectral ripples and high power intensity in ASE spectrum is required. The ASE from Er ions in silica glass covers the spectral range of 1520–1560nm via transition from $^4I_{13/2}$ to $^4I_{15/2}$. Its effective bandwidth, however, could be narrower due to non-uniform nature of the ASE and external filters which are often required for spectral uniformity. Certainly, broadband output spectrum of ASE ranging from C-band to L-band in silica fibre has been demonstrated using relatively complicated experimental setups which always were based on two-stage or two-pump sources (LDs).[10–14] The Er^{3+}-doped tellurite fibre (EDTF) has much better gain flatness and broader amplification range com-

*Project supported by the Optical Science and Technology Foundation of Shanghai (Grant No 022261046), National Natural Science Foundation of China (Grant No 60207006), and the Shanghai "Qimingxing" Project (Grant No 04QMX1448).
†E-mail: dsx@laserglass.com.cn

pared with the silica-based one.[1–4] Therefore, EDTF as a erbium–earth-doped fibre can be also used as ASE sources.[15] For example, Thorlabs Co. has recently produced a broadband ASE source with bandwidth up to 80nm, which is constructed from a single Er^{3+}–tellurite fibre pumped by a single LD.

Recently, authors reported the characterization of ASE from Er^{3+} single-doped tellurite fibre.[16] Few experimental investigations on the characterization of luminescence and related properties from Er^{3+}/Yb^{3+}-codoped tellurite fibres have been carried out. In the present investigation, a tellurite fibre codoped with 20000 ppm ytterbium and 5000 ppm erbium was fabricated from the same tellurite glass by the suction casting and rod-in-tube technologies. Luminescence and related characteristics have been investigated for fibres and bulk material of Er^{3+}/Yb^{3+}-codoped tellurite glass. Tellurite glass fibres of different lengths have been also tested with different pumping power.

2. Experimental procedures

2.1. Preparation of bulk glass

A representative tellurite glass with composition of $70TeO_2$–$20ZnO$–$5La_2O_3$–$5Li_2O$ in mol% was chosen as tellurite host.[17] The glass was codoped with 20000 ppm ytterbium and 5000 ppm erbium. The purpose of the addition of Yb_2O_3 is to enhance the pumping efficiency of 980nm LD because Yb^{3+} has a much larger absorption cross-section at the pumping wavelength than Er^{3+}. The starting materials are anhydrous powders of TeO_2, ZnO, La_2O_3, Li_2O, Yb_2O_3 and Er_2O_3 with higher than 99.99% purity. Batches of 50g were melted in platinum crucibles at 850°C in an electrically heated furnace in oxidizing atmosphere. High-purity O_2 passing through platinum tube was blown into the liquid glass during melting for 10min. The glasses obtained were annealed to room temperature gradually. Samples were cut from the cast glass block, and polished to the size of 10mm × 10mm ×1 mm for the spectrum measurements.

2.2. Preform preparation and fibre drawing

A similar melting procedure, as described for bulk glass, was adopted for making core and cladding glass. The core glass was doped with the same content of ytterbium and erbium as the bulk glass. The preform was fabricated by the suction casting and rod-in-tube technologies.[17,18] During the fibre drawing procedure, the fibre was coated with a low-refractive-index (n=1.52) polymer (DSM DeSolite®3471-2-136) outer cladding to prevent mechanical fracture. An optical microscope equipped with a JVC CCD camera measured the core and cladding diameters of the fabricated fibres. The resulting fibre had a cladding diameter of 125μm, and a core diameter $D \approx 7\mu$m, and a numerical aperture (NA) of 0.2. The average background loss was measured using the cutback method, and the value was 2.0dB/m at 1310nm.

2.3. Absorption and emission spectrum measurement

The absorption spectrum of the bulk glass is recorded with a PERKIN-ELMER-LAMBDA 900UV/VIS/NIR spectrophotometer. The sample is scanned in the range 300–1650nm. The main excitation source used for fluorescence measurement is a diode laser (Limo Fb101c765, Germany) capable of providing 15W of pump light at 980nm which has fibre-coupled output of 200μm in diameter. The fluorescence spectra are measured with a JOBIN-YVON TRIAX550 fluorescence spectrometer. For fluorescence spectrum measurement, the bulk glass is positioned so that the pump beam is allowed to be incident at the edge of the sample, and the optical path of emitted light through the sample to the detector is approximately 1 mm. For fibre emission spectrum, the pump is launched at one end of the fibre and ASE spectra from the other end are detected. The beam of the pumping laser is coupled into the fibre using a precise positioning stage (M-561D, Newport), a high reflectivity mirror at 980nm is located at the end of fibre. However, incident power coupled to the tellurite fibre is estimated as nearly one order-of-magnitude lower. The same set-up is also used for the measurement of lifetimes. A mechanical chopper is used to modulate the pump, the fluorescence is detected using a fast response InGaAs detector, and the fluorescence decay curves are recorded using a Tektronix TDS3052 oscilloscope. The lifetimes are calculated by fitting an exponential function to the data.

3. Results and discussion

3.1. Absorption spectrum of bulk glass and Judd–Ofelt parameters

Figure 1 shows the absorption spectrum of the bulk glass over a spectral range of 350–1650nm. Assignments of the absorption bands are shown by the excited levels. The intense absorption of the $^2F_{5/2}$ of

Yb^{3+} overlaps the absorption of the $^4I_{11/2}$ of Er^{3+} at the wavelength region 900 to 1000nm.

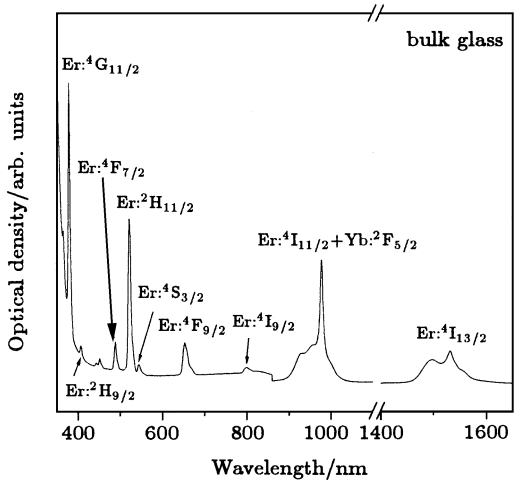


Fig.1. Absorption spectrum of the bulk glass.

The Judd–Ofelt (J-O) theory is often applied to determine the important spectroscopic and laser parameters of rare-earth-doped glasses or crystals.[19,20] According to the J-O theory, the line strength for the electric dipole transition between an initial J manifold $|(S,L)J\rangle$ and a final J' manifold $|(S',L')J'\rangle$ is given by[21]

$$S^{\mathrm{ed}}[(S,L)J;(S',L')J'] = \sum_{t=2,4,6} \Omega_t |\langle (SL)J\|U^{(t)}\|(S'L')J'\rangle|^2, \qquad (1)$$

where the three terms $\langle\|U^{(t)}\|\rangle$ are the reduced matrix elements of the unit tensor operators calculated in the intermediate-coupling approximation, and the parameters Ω_2, Ω_4, and Ω_6 are the intensity parameters which contain the effects of the crystal-field terms, radial integral of an electron, and so on. Since the reduced matrix elements $\langle\|U^{(t)}\|\rangle$ are constant characteristics to each transition, the three Ω_t (t=2, 4, 6) parameters can be obtained experimentally from the line strengths of at least three absorption bands using a least squares fitting. The three parameters Ω_t (t=2, 4, 6) of Er^{3+}in glasses are shown in Table 1.

Table 1. J-O parameters.

Glass	J-O parameters (10^{-20}cm^2)±10%			
	Ω_2	Ω_4	Ω_6	RMS
	4.42	1.34	0.76	5.3%

Using the Ω_t (t=2, 4, 6) parameters, the spontaneous emission probabilities for electric dipole transitions from the J' manifold $|(S',L')J'\rangle$ to the terminal manifold $|(S,L)J\rangle$ can be calculated by[22]

$$A[(S',L')J';(S,L)J] = \frac{64\pi^4 e^2}{3h\lambda^3(2J+1)} \times (\chi_{\mathrm{ed}} S^{\mathrm{ed}} + \chi_{\mathrm{md}} S^{\mathrm{md}}), \qquad (2)$$

where the χ terms correct the effective field at a localized center in a medium of isotropic index n and are given by $\chi_{\mathrm{ed}} = n(n^2+2)^2/9$ for electric dipole transitions and $\chi_{\mathrm{md}} = n^3$ for magnetic dipole transitions. For a transition including magnetic dipole contribution, $S^{\mathrm{md}}_{J'J}$ is given by[22]

$$S^{\mathrm{md}}[(S',L')J';(S,L)J] = \frac{1}{4m^2c^2} |< (S',L')J'\|L+2J\|(S,L)J|^2. \qquad (3)$$

Radiative electric dipole- and magnetic dipole-induced transition probabilities (denoted as A_{ed} and A_{md}, respectively), the total spontaneous emission probability A_{total}, and radiative lifetime τ_{rad} were calculated and are listed in Table 2.

Table 2. Electric and magnetic dipole induced radiative transition probabilities (denoted as A_{ed} and A_{md}, respectively), total spontaneous emission probabilities A_{total}, radiative lifetimes τ_{rad} of Er^{3+}: $^4I_{13/2} \rightarrow {}^4I_{15/2}$ transition.

Glass	Transition probility/s^{-1}			τ_{rad}/ms
	A_{ed}	A_{md}	A_{total}	
	201	62	263	3.8

3.2. Fluorescence emission spectra of the bulk and fibres

Figure 2 shows the normalized emission spectrum of the bulk glass and fibres with different lengths originating from the Er^{3+}: $^4I_{13/2} \rightarrow {}^4I_{15/2}$ transition. In the case of the bulk glass, the peak wavelength and the full width at half maximum (FWHM) are ~1532nm and ~55nm, respectively. The value of FWHM is similar to those of other tellurite glasses,[17,23] and is very large compared with those of silicate and phosphate glasses.[7] The general features of the fibres in Fig.2 are similar to those observed for the bulk glass. However, there are three notable differences in the ASE spectrum (Fig.2) of the fibres compared with the bulk glass. Firstly, the emission spectrum from erbium in fibres is almost twice as broad as the corresponding spectrum in bulk glass. For example, the FWHM is approximately 53nm for bulk glass, and 102nm for a 60cm fibre. Secondly, the peak of 1530nm that corresponds to the transition between the lowest stark levels of the $^4I_{13/2}$ and $^4I_{15/2}$ gradually disappears, and these emission peaks shift toward longer wavelength from 1558nm to 1590nm. Thirdly, the shapes of ASE

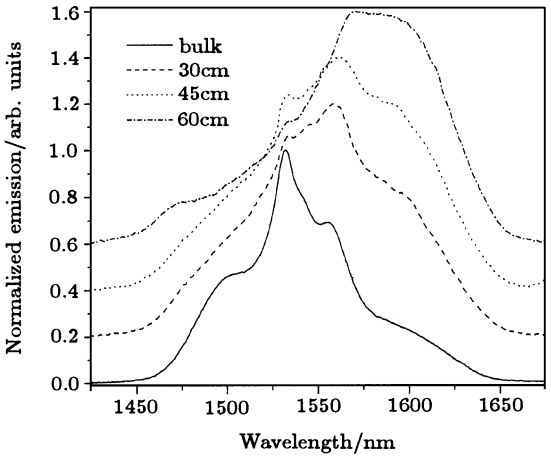


Fig.2. The normalized emission spectrum of Er^{3+}/Yb^{3+}-codoped tellurite bulk glass and fibres.

spectra for fibres apparently become broad and flattened by increasing the fibre length, especially at L-band. This is attributed to typical characteristics of a three level system, mainly the re-absorption of emission by the ground state. We can expect that fibres of longer length with the proposed Er^{3+}/Yb^{3+}-codoping concentration are more suitable to achieve a flatter broadband ASE source.

ASE spectra from fibre of 20 and 30cm lengths were also measured at different pump powers. The results are shown in Fig.3 (a) and (b), respectively. In the case of the 30cm fibre, three spectra exhibit similar features. However, these features are noticed to shift to longer wavelengths with increasing pump power. Sample of 45cm length have similar spectral features as that of 30cm length. The most interesting observation in the case of 45cm fibre is that resonance lines appear on the top of the ASE band when the pump power was increased to 400mW. Under this condition, the ASE spectrum abruptly becomes narrow. This phenomenon is clearly due to successive back-reflections from the ends of tellurite fibre sample, the large refractive index difference between the tellurite fibre (≈2.0) and the spliced silica fibres enhancing Fresnel reflection.[14]

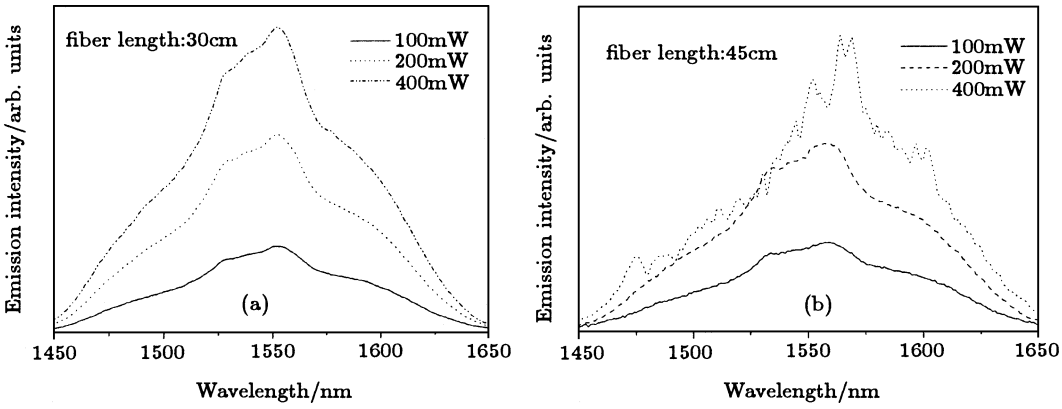


Fig.3. The ASE spectra of the fibres for various pump power. (a) 30cm; (b) 45cm.

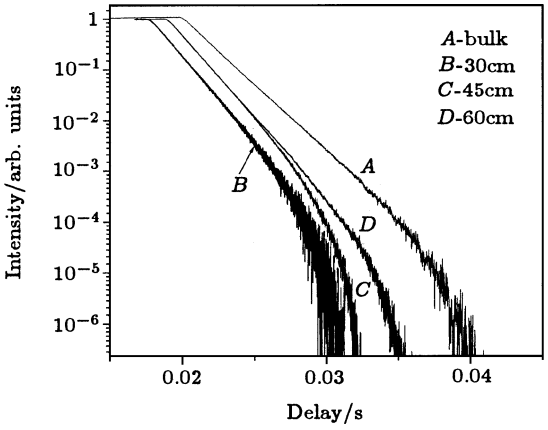


Fig.4. Fluorescence decay profile of Er^{3+}/Yb^{3+}-codoped tellurite bulk glass and fibres.

Figure 4 presents the fluorescence decay of the tellurite glass and fibres. The fluorescence intensity I versus the time t was approximated numerically by the following function:

$$I = I_0 \exp\left(-\frac{t}{\tau}\right), \tag{4}$$

where I_0 is the initial intensity and τ the fluorescence decay time.

The decay trace of the $^4I_{13/2}$ level in the bulk glass shows a nearly exponential behavior with a e^{-1} folding lifetime of ~3.6 ms, whereas the radiative lifetime (τ_{rad}) obtained from the J-O theory is about 3.8ms (shown in Table 2.). The fluorescence decay times of the bulk glass and fibres are listed in Table

3. There is a definite tendency for the fibres that the fluorescence lifetime is prolonged with increasing fibre length. However, lifetime change is small (less than 5 %) for fibre length up to 60cm. The quantum efficiency η of the luminescence from the $^4I_{13/2}$ level is determined from $\eta = \tau_{exp}/\tau_{rad}$.[24] Quantum efficiencies η of 94% and 87% are found for the metastable $^4I_{13/2}$ level in the bulk glass and fibre of 60cm length, respectively. Fluorescence lifetimes for the $^4I_{13/2} \rightarrow ^4I_{15/2}$ transitions of Er^{3+} ions in fibres are shorter than that of the bulk glass before fibre drawing. This difference indicates that contamination or OH^- content in atmosphere was introduced during the fibre drawing process.[25]

Table 3. The fluorescence decay lifetimes of the level $^4I_{13/2}$ (τ_{exp}) in the investigated bulk and fibres.

	Bulk glass	Fibre (30cm)	Fibre (45cm)	Fibre (60cm)
Fluorescence decay time/ms	3.60±0.01	3.06±0.01	3.10±0.01	3.12±0.01

3.3. Upconversion fluorescence emission spectra of the bulk and fibres

Figure 5 illustrates the upconversion spectra of the bulk glass and fibres in the range of 500–700nm under 980nm excitation. In the case of the bulk glass, the upconversion spectrum showed three bands centred around 656, 546 and 524nm, corresponding to Er^{3+} :$^4F_{9/2} \rightarrow ^4I_{15/2}$, Er^{3+} :$^4S_{3/2} \rightarrow ^4I_{15/2}$ and Er^{3+} :$^2H_{11/2} \rightarrow ^4I_{15/2}$, respectively.[22] Fig.6 shows a schematic diagram of the energy levels of Er^{3+} and Yb^{3+} ions as well as some possible mechanisms present in the process of upconversion light. The excitation process for the above three transitions can be explained as follows.[22,23] Firstly, ground state ($^4I_{15/2}$) ions are excited to the $^4I_{11/2}$ level by the processed as follows as: ground state absorption (GSA) expressed as $^4I_{15/2}+h\nu \rightarrow ^4I_{11/2}$ and the energy transfer (ET) from Yb^{3+} expressed as Er^{3+} :$^4I_{15/2}$ $+Yb^{3+}$:$^2F_{5/2} \rightarrow Er^{3+}$:$^4I_{11/2}+Yb^{3+}$:$^2F_{7/2}$, the latter is dominating due to the larger absorption cross section of Yb^{3+} than that of Er^{3+} at the pumping band range. Secondly, the Er^{3+} ion in the populated $^4I_{11/2}$ level decay to the $^4I_{13/2}$ level, these ions on $^4I_{11/2}$ and $^4I_{13/2}$ level are re-excited to the $^2H_{11/2}$ and $^4F_{9/2}$ level by excited state absorption (ESA), respectively. Thirdly, some of them on $^2H_{11/2}$ level decay to the $^4S_{3/2}$ level. The $^2H_{11/2} \rightarrow ^4I_{15/2}$ and $S_{3/2} \rightarrow ^4I_{15/2}$ transitions emit the green fluorescence of 524nm and 546nm in wavelength, respectively. The $^4F_{9/2} \rightarrow ^4I_{15/2}$ transition emits the red fluorescence of 656nm in wavelength. In the case of bulk glass, the peak emission excitation intensity ratio for the 656, 546 and 524nm emissions was determined to be 2:4.5:1.

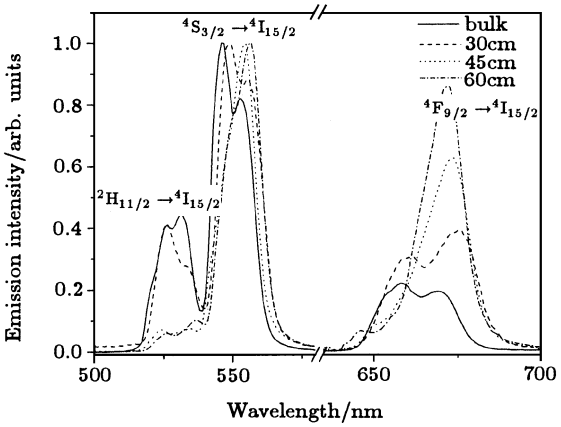


Fig.5. The normalized upconversion emission spectra of the bulk glass and fibres.

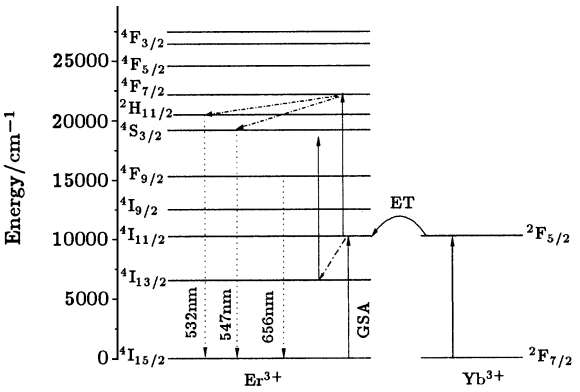


Fig.6. Schematic energy levels diagram of the Er^{3+} and Yb^{3+} for upconversion of light.

The general features of upconversion emission spectra for fibres in Fig.5 are similar to those observed for bulk glass. However, the centre of the spectrum shift toward longer wavelength with increasing fibre length is clearly seen in the three different length fibres given in Fig.5. There is a definite tendency for the relative of the 656nm emission to increase with increasing fibre length from to 30 to 60cm. For example,

the ratio of the 656 to 546nm emission peak intensities was measured to be approximately 1:2.6 for a 30cm fibre, while 1:1.1 for a 60cm fibre. Another interesting aspect observed in the fibres is that with increasing fibre length from 30 to 60cm, the intensity of the $^2H_{11/2} \rightarrow ^4I_{15/2}$ transition is drastically reduced since the $^2H_{11/2}$ level is thermally populated.[26] Finally, it is necessary to point out that the upconversion process in bulk and fibres was so efficient that the green emission could readily be seen with the naked eye, at pump power as low as a few tens of milliwatts.

3.4. Discrepancy between the bulk glass and fibres

To our knowledge, the emission spectrum from erbium in Er^{3+}/Yb^{3+}-codoped tellurite fibres having almost twice as broad as that of the corresponding spectrum in bulk glass in our results is a new phenomenon. A reasonable interpretation of our results is that there exists a strong radiation trapping among Er^{3+} ions in Er^{3+}/Yb^{3+}-codoped tellurite fibres. The radiation trapping in rare earth doped solid materials can cause the significant broadening of the emission spectrum.[27] Radiation trapping simply refers to the reabsorption and re-emission of photons due to the finite sample size and doping concentration. Therefore, it will occur along the fibre. The fraction of radiation trapping, $f_{\rm trap}$, is a parameter used frequently as a measure of radiation trapping effect. It can be calculated by[27]

$$f_{\rm trap} = \Omega_{1532}[1 - \exp(-N_{\rm Er}\sigma_{1532}V^{1/3})], \qquad (5)$$

where Ω_{1532} is the fractional spectral overlap of the absorption and emission cross-sections of the $^4I_{13/2} \rightarrow ^4I_{15/2}$ transition of Er^{3+} ions. N_{Er} and σ_{1532} are the Er^{3+} concentration and the absorption cross-section at 1532nm, respectively. $V^{1/3}$ is taken as a characteristic length proportional to the cube root of the sample pumped point volume V. It is well known that the values of σ_{1532} in tellurite glasses are always larger than that in other oxide glasses.[7] According to Eq.(5), the tellurite fibre with longer length compared with the thickness of bulk will result in a high $f_{\rm trap}$. Consequentially, the radiation trapping in longer fibre is more vigorous than that in the bulk.

In the case of the fibres, there is a distinct tendency for the fluorescence lifetime to become longer, and for the peak emission wavelength to shift toward longer wavelength with increasing fibre length. These are also naturally expected as the results of radiative trapping due to reabsorption of Er^{3+} emission. However, the former effect was clearly observed for Er^{3+}/Yb^{3+}-codoped tellurite glass fibre and only slightly in Er^{3+}-single doped tellurite, which we have reported previously.[16] This effect seems to be due to the introduction of Yb^{3+} ions into Er^{3+}-doped tellurite glass. The precise mechanism is not known. One possible mechanism is as follows: upon the introduction of ytterbium ions to Er^{3+}-doped tellurite glasses, the absorption efficiency at 980nm is enhanced by energy transfer process $Er^{3+}:^4I_{15/2} + Yb^{3+}:^2F_{5/2} \rightarrow Er^{3+}:^4I_{11/2} + Yb^{3+}:^2F_{7/2}$. This leads to the pump light being transmitted longer along the fibre as long as the pump light is not completely absorbed. The results under this condition will cause more Er^{3+} ions to be involved in the pump process.

4. Conclusions

We have fabricated Er^{3+}/Yb^{3+}-codoped tellurite glass and fibres. The measured absorption spectrum of bulk glass was analysed by J-O theory and the Ω_t (t=2, 4, 6) parameters were estimated. Radiative transition rates of Er^{3+}: $^4I_{13/2} \rightarrow ^4I_{15/2}$ transition in bulk were calculated and a comparison between the experimentally measured lifetimes and the calculated ones gave a quantum efficiency of 94 % and 85 % for the metastable $^4I_{13/2}$ level in the bulk glass and fibre of 30cm length, respectively. Both IR and upconversion VIS emission of light of the bulk and fibres were investigated. In the case of the fibres, a nearly ~200nm broad erbium ASE in the 1450nm to 1650nm range is observed around 1.53μm when pumped at 980nm and, at sufficiently high pump powers, resonance lines are also seen at the peak of the ASE curve. The additional effect of radiation trapping due to the reabsorption results in significant broadening of the emission spectrum in fibres compared with bulk glass. The Er^{3+}/Yb^{3+}-codoped tellurite fibres will be useful for efficient 980nm pumped broadband Er^{3+}-doped fibre amplifiers and tunable fibre lasers.

References

[1] Mori A, Ohishi Y and Sudo S 1997 *Electron. Lett.* **33** 863

[2] Ono H, Mori A, Shikano K and Shimizu M 2002 *IEEE Photon. Technol. Lett.* **14** 1070

[3] Ono H, Mori A, Shikano K and Shimizu M 2002 *IEEE Photon. Technol. Lett.* **14** 1073

[4] Yang J, Dai N, Dai S, Yang Z, Xu S, Hu L and Jiang Z 2003 *Chin. Phys.* **12** 669

[5] Tokuda Y, Saito M, Takahashi M, Yamada K, Watanae W, ItohK and Yoko T 2003 *J.Non-Cryst.* **326**&**327** 472

[6] Martina M, Caricato A P, Fernandez M, Leggieri G, Jha A, Ferrari M and Mattarelli M 2003 *Thin Solid Films* **433** 39

[7] Ivan P K and Ting L 2002 *Optical Fiber Telecommunications IVA Components* (San Diego, CA: Academic) chap3. p119

[8] Leberdev V A, Pisarenko V F, Chuev Y M, Perliflin A A, Avanesov A G, Zhorin V V, Okhrimchuk A G and Shestakov A V 1997 *J. Lumin.* **72**&**74** 942

[9] Hu Y, Jiang S, Sorbello G, Luo T, Ding Y, Hwang B C, Kim J H, Seo H J and Peyghambarian 2001 *Proc. SPIE* **4282** 57

[10] Aozaso S, Sakamoto T, Kanamori T, Hoshino Kobayashi K and Shimizu M 2001 *IEEE Photon. Technol. Lett.* **12** 1331

[11] Jeong H,Oh K, Han S R and Morse T 2003 *Chem. Phys. Lett.* **367** 507

[12] Huang W, Tam H, Wai P, Dong X, Hai M and Xie J 2002 *Chin. Phys. Lett.* **19** 1307

[13] Zhang H, Wu J and Gao J 2003 *Chin. Phys.* **12** 178

[14] Espindola P, Ales G, Park J and Strasser T 2000 *Electron. Lett.* **34** 1263

[15] Marjanovic S, Toulouse J, Jain H, Sandmann C, Dierolf V, Kortan A, Kopylov N and Ahrens R 2003 *J. Non-Cryst.* **322** 311

[16] Dai S, Zhang J, Li S, Hu L and Jiang Z 2004 *Chin. Phys. Lett.* **21** 329

[17] Wang J S, Vogel E M and Snitzer E 1994 *Opt. Mater.* **3** 187

[18] Kanamori T, Terunuma Y, Nishida Y, Hoshino K, Nakagawa K, Ohishi Y and Sudo S 1997 *J. Non-Cryst.* **213**&**214** 121

[19] Judd B R 1962 *Phys. Rev.* **127** 750

[20] Ofelt G S 1962 *J. Chem. Phys.* **37** 511

[21] Feng X, Tanabe S and Hanada T 2001 *J. Am. Ceram. Soc.* **84** 165

[22] Tanabe S 1999 *J. Non-Cryst.* **259** 1

[23] Ding Y, Jiang S, Hwang B, Luo T, Peyghambarian N and Miura Y 1999 *Proc. SPIE* **3622** 166

[24] Rolli R, Montagna M, Chaussedent S, Monteil A, Tikhomirov V K and Ferrari M 2003 *Optical Materials* **21** 743

[25] Jiang S, Luo T, Hwang B C, Smekatala F, Seneschal K, Lucas J and Peyghambarian N 2003 *J. Non-Cryst.* **263**&**264** 364

[26] Chamarro M A and Cases R 1990 *J. Lumin.* **46** 59

[27] Ehrmann P R and Campbell J H 2002 *J. Am. Ceram. Soc.* **85** 1061